WiLi - Vehicular Wireless Channel Dataset enriched with LiDAR and Radar Data

Benjamin Rainer[1], Stefan Zelenbaba[1], Anja Dakić[1], Markus Hofer[1], David Löschenbrand[1], Thomas Zemen[1], Xiaochun Ye[2], Guo Nan[2], Stefan Teschl[3], Peter Priller[3]
[1] Austrian Institute of Technology GmbH, Giefinggasse 4, 1210 Vienna, Austria
[2] Institute of Computing Technology, CAS, Bejing, China
[3] AVL List GmbH , Hans-List-Platz 1, 8020 Graz, Austria

***Abstract*—This paper discusses a freely available and open dataset containing vehicle-to-vehicle (V2V), vehicle-to-infrastructure (V2I) and vehicle-to-pedestrian (V2P) OFDM-based wireless channel measurement data including synchronised sensor data such as radar, LiDAR and high precision GPS. The wireless channel measurement is conducted at the carrier frequencies of 3.2 GHz and 5.81 GHz which are the most promising frequency bands in which future V2X communication systems will operate. The dataset contains the wireless channel measurement data of various V2X scenarios along with synchronized sensor information from a vehicle. In addition to the wireless channel measurement data, the dataset also includes frame error rate measurements from a IEEE 802.11p based communication system, synchronized to the other measurement data.**

I. Introduction

Recent research with respect to autonomous driving heavily focuses on recognizing the environment by using sensors of all type, such as video, LiDAR, radar, etc. A lot of effort is invested in deducing facts from the sensor data: perception algorithms fuse sensor information, detect and describe relevant objects (e.g., road participants). This is used by path planning algorithms, fueling into control algorithms taking *driving decisions* [1]. Recent advances show that these efforts are bearing fruits and that we are getting closer to self-driving vehicles [2]. However, wireless communication has only been seen as a method to provide to and collect data from vehicles but it has not been deemed as a crucial ingredient towards self-driving vehicles.

This view has changed in the last years and [3] exemplary shows that communication between vehicles (V2V) and between vehicles and infrastructure (V2I) can be beneficial in solving some of the remaining challenges [4], like predicting future behavior of nearby objects, which in turn requires robust perception also under unfavorable conditions (e.g., bad weather or occlusion). Data collected from other road users can help in decision finding and may help in cross-validating acquired facts or trained models. Wireless communication enables the vehicle's to take into account data, models, and facts from other road users which potentially can lead to an increased road safety. Leaving aside security issues, this puts enormous requirements on the underlying wireless communication links/channels with respect to latency, reliability and bandwidth. Mission critical data has to be sent via reliable communication protocols which in-turn induce latency if the underlying physical medium is error prone. In order to test and validate the capabilities of V2X communication for (semi-)autonomous vehicles, datasets that provide sensor data (LiDAR, radar, etc.) from real scenarios are readily available [5]. But, in order to test and validate the decision making processes of such (semi-)autonomous vehicles information about the wireless communication links is crucial.

In this paper we discuss and publicly provide the WiLi dataset under the Creative Commons license. Our dataset goes beyond the state of the art LiDAR datasets. We do not only provide high resolution LiDAR data for realistic V2X scenarios (urban inner city scenarios) but also synchronized, to the LiDAR data, OFDM-based wireless channel sounding data at 3.2 GHz and 5.81 GHz enriched with the frame error rates of a IEEE 802.11p wireless communication including precise GPS positioning information. This allows a rigorous study of what the sensors of a (semi-)autonomous vehicle perceive including accurate wireless channel measurements.

The scientific contribution of this paper are:

- discussion of the measurement system and dataset details;
- provide an overview on the measured scenarios and first insights on the gathered data.

II. Measurement System

The measurement campaign is designed to provide a comprehensive dataset describing the environment and radio channel properties in safety critical urban scenarios. For measuring the radio channel, we use the AIT OFDM-based multi-band channel sounder [6], capable of sounding up to three wireless channels within three different frequency bands simultaneously. For this dataset we record two wireless channels, the first in the 3.2 GHz band at the very same carrier frequency and the second channel in the 5.9 GHz band at a carrier frequency of 5.81 GHz. We sound the channels with an effective bandwidth of 150.25 MHz, respectively, having 601 subcarriers with a spacing of 250 kHz. The omnidirectional antennas for the different frequency bands were mounted on the roof of the ego vehicle. The selected frequencies have been

978-1-6654-3540-6/22

Fig. 1: Measurement vehicles, left the AIT vehicle with the receiver equipment and an MK5 OBU. On the right the AVL vehicle (ego vehicle) equipped with two LiDARs, a 128 beam LiDAR in the front and a 32 beam LiDAR in the back. The rear and front bumper are equipped with radar.

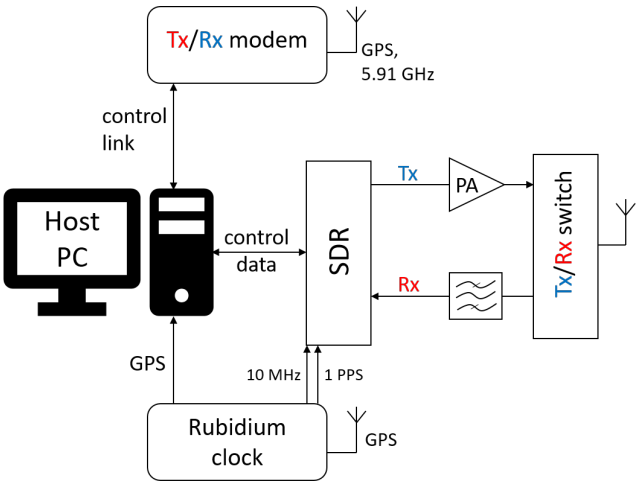

Fig. 2: Measurement setup including AIT multi-node/multi-band channel sounder and Cohda Wireless MK5 modems.

chosen with the envisioned wireless communication standards for V2X communication in mind (e.g., 802.11p, PC5). In addition to the wireless channel, we also record LiDAR and radar data of the environment. This data is recorded synchronously to the wireless channel data. Figure 1 depicts the two measurement vehicles and the mounting positions of the antennas, LiDAR, and radar sensors. For environmental perception, the ego vehicle was equipped with a Ground Truth Reference System (GTRS) from AVL. It consists of two differential GPS antennas combined with two LiDAR sensors (one Velodyne Ultra Puck VLP-32c supporting 32 beams in the back, plus one Ouster OS2-128 with 128 beams covering the front) mounted in a rooftop-box (RTB) about 1.47 m above street level. The front and the rear bumper were each equipped with a Conti ARS408-21 smart radar. Video cameras were available, but footage was not included in the data set to avoid potential breaches of privacy legislation. Precise localization was done using a Reach RS2 Multi-band RTK GNSS Receiver as GPS plus IMU sensors, connected to a Novatel GNSS-802 antenna. The integrated in-vehicle processing system pre-processes and synchronizes data, which is then streamed to mass storage (SSD).

In addition to the wireless channel sounding, LiDar and radar data, we also include the results from Cohda Wireless MK5 on-board unit (OBU) modems which are based on IEEE 802.11p PHY [7]. The modems are used to obtain the frame error rate (FER) directly on the road. Both modems, the transmitter (Tx) and the receiver (Rx), are equipped with the GPS Multi-band Surface Mount Antenna, which combines two 5.9 GHz antennas with one GPS antenna. In our scenario, we use one 5.9 GHz antenna and one GPS antenna. Since every node of the AITs' multi-band channel sounder is also connected to the GPS antennas, we synchronize them via GPS to the Tx and the Rx modems. The schematic of the measurement setup which includes a single AIT channel sounding node and the Cohda Wireless MK5 OBU is shown in Figure 2. The modem is connected via ethernet to the host PC of the node, where LabView Communications is used to control the sounding and the execution of transmit commands (Tx modem) or reception commands (Rx modem). The node selected as the transmitter is connected to the Rx modem (referred as red color in Figure 2) and the receiving channel sounder node is connected to the Tx modem (referred as blue color in Figure 2).

The number of the transmitted frames between the MK5 OBUs is set according to the time needed for each scenario considering a frame rate of 1500 frames/s. For each scenario we use a quadrature phase shift keying (QPSK) modulation with a coding rate of 1/2 and 64-quadrature amplitude modulation (64QAM) with a coding rate of 3/4. The report file of the Rx modem contains information about the GPS time and coordinates, the sequence number, as well as the power and the noise level of each received frame. To evaluate the FER results, we split the report file into multiple time windows, each of a size of $T_{\text{period}} = 1$ sec. The FER is then given as the ratio of the number of the missing frames and the transmitted frames within a time window.

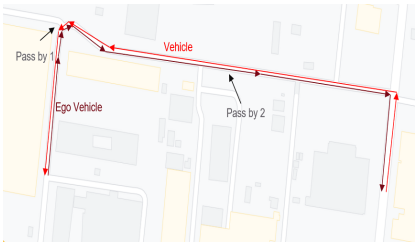

(a) V2V wireless communication scenario where the vehicles pass by each other at the passing by points.

(b) V2V wireless communication scenario on a four lane road which narrows down to two lanes.

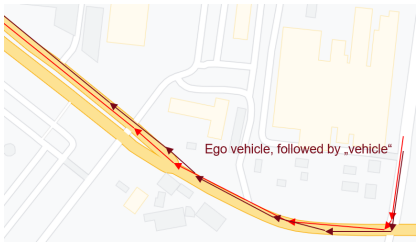

(c) V2V wireless communication scenario where one vehicle follows the ego vehicle with different gap sizes.

Fig. 3: V2V wireless communication scenarios where the passing points indicate where the vehicles passed by in different measurement runs.

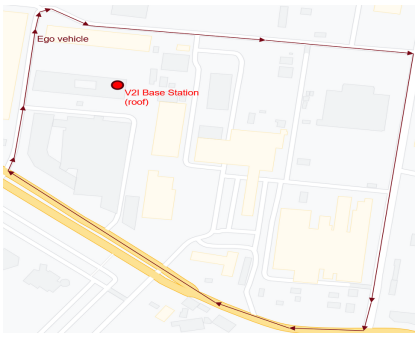

(a) V2I wireless communication scenario where the infrastructure node is placed on a roof.

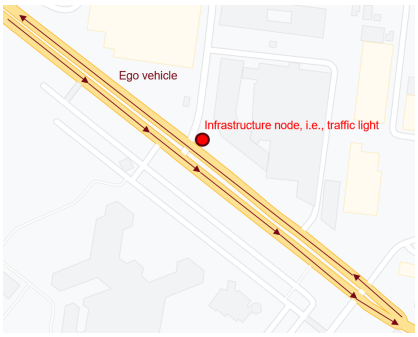

(b) V2I wireless communication scenario where the infrastructure node is a traffic light.

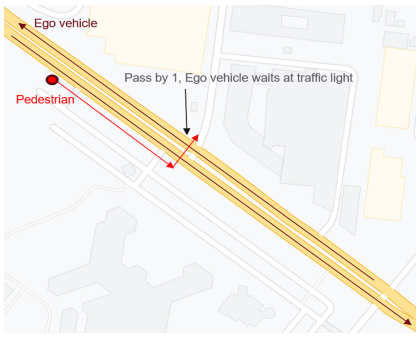

(c) V2P wireless communication scenario where the pedestrian(s) are walking parallel to the road.

Fig. 4: V2I & V2P wireless communication scenarios with different types and positions (height) of the infrastructure node.

Scenario	Length	No. Runs	Modulation (Runs)	Max Vel.	Weather	MK5 TX	3.2 GHz	5.81 GHz
V2V Scenario 1, P1	45s	21	QPSK (10), 64QAM (11)	30 km/h	light rain	20 dBm	-10 dBm	0 dBm
V2V Scenario 1, P2	45s	21	QPSK (11), 64QAM (10)	30 km/h	light rain	20 dBm	-10 dBm	0 dBm
V2V Scenario 2	80s	23	QPSK (17), 64QAM (4)	50 km/h	cloudy	20 dBm	-10 dBm	0 dBm
V2V Scenario 3	130s	15	QPSK (17), 64QAM (4)	50 km/h	cloudy	20 dBm	-10 dBm	0 dBm
V2P Scenario	49s	28	QPSK (18), 64QAM (10)	50 km/h	cloudy	20 dBm	-10 dBm	0 dBm
V2I Scenario 1	450s	2	QPSK	50 km/h	clear	20 dBm	20 dBm	20 dBm
V2I Scenario 2	40s	22	QPSK (10), 64QAM (12)	50 km/h	clear	20 dBm	-10 dBm	0 dBm

TABLE I: Dataset and scenario details.

III. Scenarios

We measured six different V2X scenarios including V2V, V2I and V2P scenarios. The scenarios were measured at the AIT Campus in Vienna (GPS location: 48.26934344779893, 16.426617202616217). We distinguish six types of the scenarios: V2V small road (cf. Figure 3a), V2V four-lane road (cf. Figure 3b), V2V follow me scenario (cf. Figure 3c), V2I base station scenario (cf. Figure 4a), V2I traffic sign scenario (cf. Figure 4b) and V2P scenario (cf. Figure 4c). The V2V scenario consists of two sub-scenarios. The first covers the small road, and a situation where the two vehicles approach each other. In this case the velocity of the vehicles is limited to 30 km/h (according to speed limits) and the measurements runs are repeated for the indicated passing points (cf. Figure 3a). The second sub-scenario is performed on a four-lane road where the vehicles approach each other at a maximum velocity of 50 km/h (cf. Figure 3b). The third sub-scenario was also on a four-lane road (cf. Figure 3c), but this time one vehicle is driving behind the ego vehicle and we performed different measurements runs with the different gaps between the two vehicles. The V2I scenario targets the case where vehicles exchange safety critical information with a base station or infrastructure node on an elevated position. In the first case the infrastructure node is mounted on the roof of the AIT building, and the ego vehicle drives around the AIT campus (cf. Figure 4a). In the other case, the infrastructure node was mounted at a traffic crossing imitating a smart traffic light or sign (cf. Figure 4b). The last scenario depicts a V2P scenario, where the vehicle is exchanging information with a smart device carried by pedestrians. In this scenario, the pedestrian is travelling parallel to the road lanes and then crossing the road at an intersection, while the ego vehicle is passing and waiting at the crossing, respectively (cf. Figure 4c).

Rx Time [s]	Rx TS [s]	Lat [deg]	Lon [deg]	Head [deg]	Speed [mps]	Size [byte]	Src Start	Seq. Nr.	Src Lat [deg]	Src Lon [deg]	Src Head [deg]	Src Speed [mps]	RSSI A [dbm]	Noise A [dbm]
16381954 54.80953	16381954 54.70604	48 .26904	16 .426464	1.5	5.64	54	154	120	48.26 9683	16.42 8606	276.8	11.3	-94	-102

TABLE II: Example of an MK5 OBU Rx log entry.

IV. Dataset Organization

The dataset is organized into the previously described scenarios. For each scenario and modulation configuration (QPSK vs. 64QAM) of the MK5 OBUs we repeated the measurements. We only include those repetitions (runs) which have useful data in order to reduce the dataset size to a useful dimension. For the V2I scenario where we mimic the infrastructure node on a roof by putting our channel sounding equipment on the roof of one of the AIT buildings (Giefinggasse 4) we had to increase the transmit power of the channel sounder. Table II lists for each scenario the number of runs, used modulation for the MK5 OBUs, maximum velocity, weather and transmit power of channel sounder at different carrier frequencies such as the MK5 OBU transmit power.

For each measurement run there is radar and LiDAR data available from the ego vehicle's perspective. This data is synchronised using GPS and also the GPS coordinates are stored. Each measurement system, ego vehicle's sensors, channel sounder and MK5 OBUs store GPS data which can be used to align and correlate the data samples with each other. The LiDAR and radar data is separated into back and front, reflecting the sensor setup of the ego vehicle (cf. Figure 1). We provide the already preprocessed channel sounding results in a MATLAB compatible data structure for each scenario, run and carrier frequency. The MATLAB data structure consists of the corresponding time-varying channel transfer function and the channel sounding parameters, such as the subcarrier spacing in Hz, the number of subcarriers, repetition rate in seconds and the carrier frequency in Hz. The data gathered by the MK5 OBUs is provided as text files. The transmitter logs provide information about the sending rate, transmit power, and the total number of frames sent. An example line of the receiver log is given in Table II. GPS data is recorded in a separate text file. The LiDAR data is provided in the LAS/LAZ file format. As previously mentioned, for each measurement run the data of the front 128 beam LiDAR, mounted in the front, and the 32 beam LiDAR, mounted in the back, is provided, respectively. Additionally, the data is augmented by GPS information provided in the NMEA format.

V. Exemplary Results

We provide some exemplary results of the measurement campaign. We therefore compute the time-varying power delay profile (PDP) and the normalized time-varying Doppler spectral density (DSD) according to [8], [9] at 3.2 GHz and 5.81 GHz (cf. Figures 6a and 6b), delay, Doppler spreads and path loss (cf. Figure 5), and the FER (cf. Figure 7)

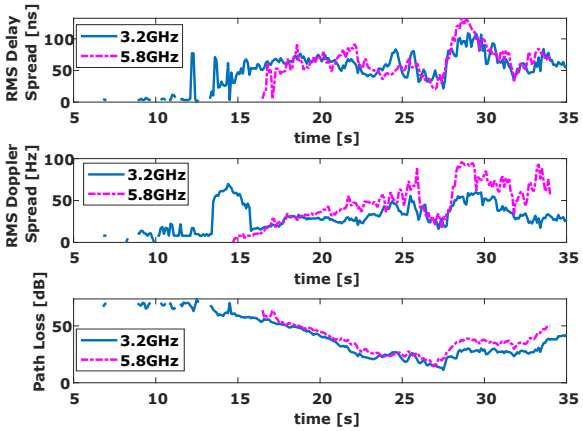

Fig. 5: Delay, Doppler spread and path loss for the two wireless communication channels at 3.2 GHz and 5.81 GHz.

for the V2V scenario for a single run and the first passing point (cf. Figure 3a). The delay and Doppler spread for the different carrier frequencies show some similarity but also bear the expected discrepancies. The path losses show a similar evolution over time which indicates that the mounting of the antennas had no significant impact on the channel measurements. For the higher carrier frequency we see that the Doppler spread is higher which is expected. The first 15 seconds of Figure 5 can be omitted as there is not much power in the channel (cf. Figures 6a and 6b) which leads to inaccurate spreads. The similarities are expected as the antennas were co-located on the roof tops on the vehicles.

The first five seconds of the FER results are omitted as the Rx modem did not receive any frames. The figures indicate that the measured time-variant channel impulse response and the FER obtained from the MK5 OBUs coincide. Figure 8 depicts a snapshot of the LiDAR data recorded during a run in the V2V scenario. The parked car besides the road, the buildings and the windows are clearly visible.

VI. Conclusion

In this paper we present a dataset which resulted from a wireless OFDM-based channel measurement campaign. The presented dataset is not yet another dataset as it includes not only wireless channel measurements but also LiDAR and radar data for all of the measured scenarios. The data of the different systems is tagged by data obtained from precise GPS systems

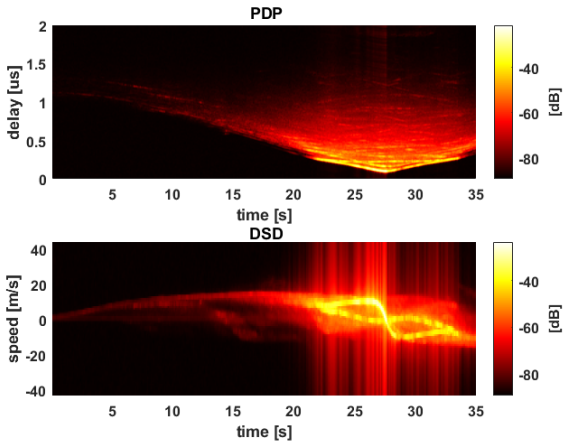

(a) Time-varying PDP and DSD for V2V scenario 1 and the first passing point for the wireless channel at a carrier frequency of 3.2 GHz.

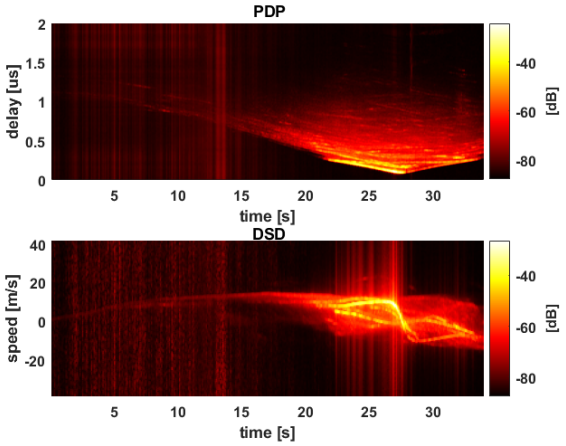

(b) Time-varying PDP and DSD for V2V scenario 1 and the first passing point for the wireless channel at a carrier frequency of 5.81 GHz.

Fig. 6: PDP and DSD of a single scenario and measurement run at a carrier frequency of 3.2 and 5.8 GHz.

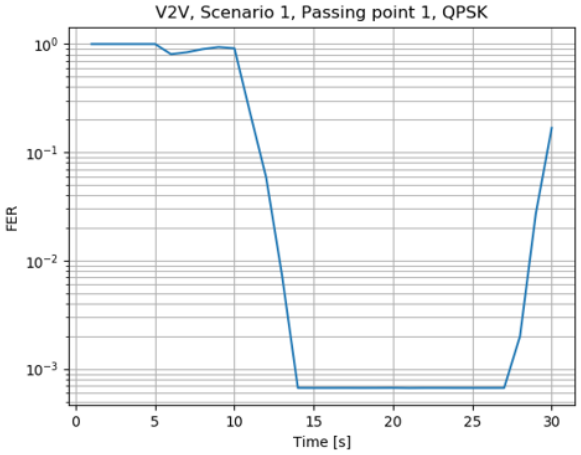

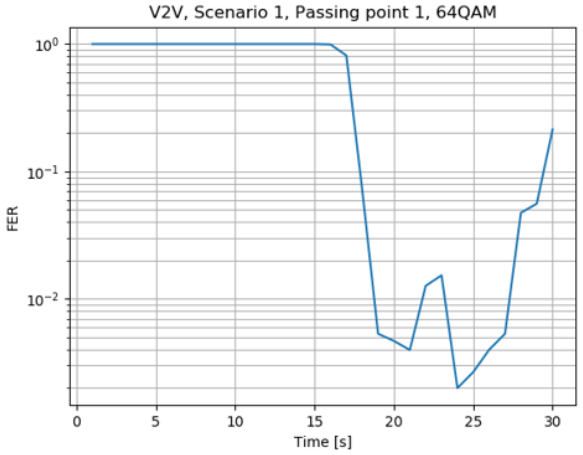

Fig. 7: Resulting FER, evaluated from the receiver log file of the MK5 OBUs, for different modulation schemes obtained for the V2V scenario 1 and the first passing point.

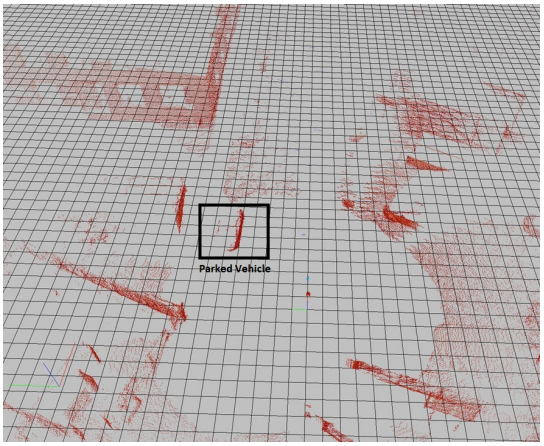

Fig. 8: Example 3D point cloud data obtained from the LiDAR sensors during V2V scenario 1.

such that it can be easily synchronized and correlated. The dataset is available at https://project-relevance.org/.

VII. Acknowledgments

This work is funded by the Austrian Research Promotion Agency (FFG) and the Austrian Ministry for Transport, Innovation and Technology (BMK) within the project RELEVANCE (881701) of the funding program transnational projects, by the European Commission within the European Union's Horizon 2020 research innovation programme funding ECSEL Joint Undertaking project AI4CSM under Grant Agreement No. 101007326 and within the project DEDICATE (Principal Scientist grant) at the AIT Austrian Institute of Technology.

REFERENCES

[1] E. Yurtsever, J. Lambert, A. Carballo, and K. Takeda, "A survey of autonomous driving: Common practices and emerging technologies," *IEEE Access*, vol. 8, pp. 58 443–58 469, 2020.

[2] I. Yaqoob, L. U. Khan, S. M. A. Kazmi, M. Imran, N. Guizani, and C. S. Hong, "Autonomous driving cars in smart cities: Recent advances, requirements, and challenges," *IEEE Network*, vol. 34, no. 1, pp. 174–181, 2020.

[3] N. Cheng, F. Lyu, J. Chen, W. Xu, H. Zhou, S. Zhang, and X. Shen, "Big data driven vehicular networks," *IEEE Network*, vol. 32, no. 6, pp. 160–167, 2018.

[4] N. Marko, E. Möhlmann, D. Ničković, J. Niehaus, P. Priller, and M. Rooker, "Challenges of engineering safe and secure highly automated vehicles," *arXiv preprint arXiv:2103.03544*, 2021.

[5] "PandaSet: Public large-scale dataset for autonomous driving." Available: https://scale.com/open-datasets/pandaset, accessed: 2021-05-26.

[6] M. Hofer, D. Löschenbrand, J. Blumenstein, H. Groll, S. Zelenbaba, B. Rainer, L. Bernadó, J. Vychodil, T. Mikulasek, E. Zöchmann, S. Sangodoyin, H. Hammoud, B. Schrenk, R. Langwieser, S. Pratschner, A. Prokes, A. F. Molisch, C. F. Mecklenbräuker, and T. Zemen, "Wireless vehicular multiband measurements in centimeterwave and millimeterwave bands," in *2021 IEEE 32nd Annual International Symposium on Personal, Indoor and Mobile Radio Communications (PIMRC)*, 2021, pp. 836–841.

[7] IEEE, "IEEE Standard for Information technology– Local and metropolitan area networks– Specific requirements– Part 11: Wireless LAN Medium Access Control (MAC) and Physical Layer (PHY) Specifications Amendment 6: Wireless Access in Vehicular Environments," *IEEE Std 802.11p-2010 (Amendment to IEEE Std 802.11-2007 as amended by IEEE Std 802.11k-2008, IEEE Std 802.11r-2008, IEEE Std 802.11y-2008, IEEE Std 802.11n-2009, and IEEE Std 802.11w-2009)*, pp. 1–51, 2010.

[8] L. Bernadó, T. Zemen, F. Tufvesson, A. F. Molisch, and C. F. Mecklenbrauker, "Delay and Doppler spreads of nonstationary vehicular channels for safety-relevant scenarios," *IEEE Trans. Veh. Technol.*, vol. 63, no. 1, pp. 82–93, Jan. 2014.

[9] D. Slepian, "Prolate spheroidal wave functions, Fourier analysis, and uncertainty-V: The discrete case," *Bell Syst. Techn J.*, vol. 57, no. 5, pp. 1371–1430, May 1978.